Article:
Brunetti, D., Graves, J. P. orcid.org/0000-0002-7959-7959, Ham, C. J. et al. (1 more author) (2025) An explanation for hard MHD stability limits in low-q95 diverted tokamak plasmas. Plasma Physics and Controlled Fusion. 082502. ISSN: 1361-6587

https://doi.org/10.1088/1361-6587/adf997

Plasma Physics and
Controlled Fusion

LETTER • **OPEN ACCESS**

An explanation for hard MHD stability limits in low-q_{95} diverted tokamak plasmas

To cite this article: D Brunetti *et al* 2025 *Plasma Phys. Control. Fusion* **67** 082502

OPEN ACCESS
IOP Publishing

Letters
Plasma Physics and Controlled Fusion

Plasma Phys. Control. Fusion **67** (2025) 082502 (6pp)
https://doi.org/10.1088/1361-6587/adf997

Letter

An explanation for hard MHD stability limits in low-q_{95} diverted tokamak plasmas

D Brunetti[1,*], J P Graves[2,3], C J Ham[1] and S Saarelma[1]

[1] UKAEA (United Kingdom Atomic Energy Authority), Culham Campus, Abingdon, Oxfordshire OX14 3DB, United Kingdom
[2] York Plasma Institute, Department of Physics, University of York, York, Heslington YO10 5DD, United Kingdom
[3] École Polytechnique Fédérale de Lausanne (EPFL), Swiss Plasma Center (SPC), CH-1015 Lausanne, Switzerland

E-mail: daniele.brunetti@ukaea.uk

Received 3 June 2025, revised 16 July 2025
Accepted for publication 8 August 2025
Published 20 August 2025

Abstract
This paper proposes a model attempting to explain the appearance of fast growing global disruptive instabilities in diverted configurations when the safety factor near the magnetic separatrix approaches two. We show that if edge density and pressure gradients are strong enough, although external kink modes are stable, poloidal harmonics may couple allowing for a global fluid perturbation to become unstable. The instability window is approached sharply as the mode resonance occurs in the edge region, and is characterised by rather large growth rates even with modest gradients.

Keywords: MHD, stability, q_{95}, tokamak

1. Introduction

Tokamak operation is typically limited by the amount of current I_p that can flow within the plasma. For a given strength of the toroidal field, if I_p is too large, a catastrophic collapse of the plasma column is almost certain. Indeed, it is a well known fact that the lower the value of the edge safety factor q_{edge}, with q measuring the pitch of the field lines, the more difficult the machine operation.

In limited plasmas, the total current is inversely proportional to the q_{edge}: as the current increases, q_{edge} decreases passing through several m/n rationals. As a consequence, an instability of helicity m/n can be triggered, exhibiting either tearing or external kink-like nature depending on how far (or close) q_{edge} is to the rational number m/n [1, 2]. Usually, a disruptive (hard) limit is reached when q_{edge} approaches 2. For limited tokamak configurations, such behaviour can be easily explained by conjecturing that a current driven external kink mode is triggered when q_{edge} drops below 2 [1]. External kinks are global disturbances growing on Alfvénic time-scales which, to be unstable, require their associated mode resonance to occur in vacuum region, i.e. not within the plasma.

A similar phenomenology is observed in diverted geometries where, because of the divergence of q at the plasma boundary identified by the magnetic separatrix, the role of q_{edge} is taken instead by q_{95}, namely the value of q associated with the

* Author to whom any correspondence should be addressed.

surface enclosing 95% of the poloidal flux. However, invoking the onset of an external kink to explain the $q_{95} = 2$ hard limit in diverted plasmas is challenged by imposing an infinite number of $m/n > q_{95}$ resonances inside the plasma, making external kink modes intrinsically stable regardless of the current peaking which is measured by the ratio $q_{\rm edge}/q_0$ with q_0 the value of at the axis. Hence, we must devise an alternative approach for explaining such behaviour. Notice that we do not address the issue of the triggering of global magnetohydrodynamic (MHD) modes during, e.g. vertical displacement events in limited geometry [3, 4].

Contrary to the resistive analysis of [2], we develop our analysis within the ideal plasma approximation and leverage the presence of strong mass density (hereafter referred to just as density), and thus pressure, gradients in the edge region [5]. The idea is to exploit the pressure induced mode coupling occurring near the plasma boundary to allow for perturbations with kink features to develop. The resulting instability, whose onset must occur only when $q_{95} \approx 2$, is required to exhibit a global character with a fairly fast growth and indeed much faster than that predicted by a resistive model.

The letter is organised as follows: after providing the necessary information about the equilibrium plasma state we lay down the model equations accounting for the required physical mechanisms occurring in the plasma and vacuum regions. With a highly simplified, yet physically relevant profiles, we then proceed to derive the dispersion relation for a perturbation characterised by a dominant helicity. The dispersion relation is thus analysed for the specific case of $q_{95} \approx 2$, and several conclusions about parameter dependencies, mode structure are instability window are drawn. Concluding remarks are finally discussed.

2. Simplified model equilibrium

We consider a large aspect ratio circular tokamak plasma of major and minor radii R_0 and a respectively with $\varepsilon = a/R_0 \ll 1$. We employ a right handed straight field line coordinate system (r, ϑ, ϕ) where r is a flux label with the dimensions of length zero on the magnetic axis, and ϑ (counter-clockwise poloidally) and ϕ are the poloidal and toroidal angles respectively. A vacuum gap separates the plasma from an ideally conducting metallic wall located at distance $b > a$ with $b/R_0 \ll 1$. The equilibrium magnetic field is

$$\boldsymbol{B} = F\boldsymbol{\nabla}\phi - \boldsymbol{\nabla}\psi \times \boldsymbol{\nabla}\phi, \tag{1}$$

where ψ is the poloidal flux and $F \approx R_0 B_0$ with B_0 denoting the magnetic field strength on the axis. The safety factor is written as $q = \sqrt{g}F/(R^2\psi')$ with $\sqrt{g} \approx rR_0$ denoting the Jacobian. For the sake of simplicity, we introduced the notation $' \equiv {\rm d}/{\rm d}r$. To model the sharp rise of q induced by the separatrix we assume that this divergence is well localised in an infinitesimally narrow region about the boundary. Hence, away from the plasma-vacuum boundary, q is taken to be piece-wise continuous, constant for $0 < r < r_0$ (*inner region*) with value q_0 and parabolic $q = q_a(r/a)^2$ for $r_0 < r < a$ and $r > a$ (*outer region*) such that $q(r_0) = q_0$. Note that in the outer region the safety factor can also be written as $q = q_0(r/r_0)^2$. This is roughly in line with the results employed in numerical investigations of diverted plasmas [6]. The logarithmic divergence is crudely modelled by letting $q = \infty$ at $r = a$.

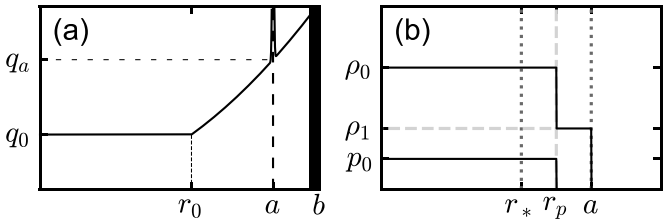

Figure 1. Safety factor (a), and pressure and density profiles (b) used in the analytic calculations. The form of p and ρ for $r < r_*$ are not required.

Normalising $\mu_0 = 1$, a low-β ordering $\beta = 2p/B_0^2 \sim \varepsilon^2$, with p the equilibrium pressure, is assumed although enhanced density and pressure gradients are allowed in the edge region which extends from r_* to a with $r_0 < r_*$. Letting ρ denote the equilibrium mass density, we assume

$$\begin{aligned} &\rho = \rho_0 \text{ and } p = p_0 \text{ for } r_* < r < r_p, \\ &\rho = \rho_1 \text{ and } p = 0 \text{ for } r_p < r < a, \end{aligned} \tag{2}$$

with $\rho_1 < \rho_0$. We take ρ_1 strictly different from zero, otherwise we would not be able to construct a finite 'plasma' solution. Here we accounted for the fact that since $p \propto \rho T$ with T the equilibrium temperature, the mass density profile is expected to be more radially extended than the pressure one. The shape of q, pressure and density profiles just described is depicted in figure 1. We point out that mathematical manipulations are highly simplified by such a choice of the equilibrium profiles, yet retaining many physically relevant elements. This is because stability properties will be seen to depend on quantities which are integrated over the region of strong gradients, so that the Heaviside nature of figure 1 will be effectively smoothed out. Hence, having described the basic features of our model tokamak equilibrium, we can divert now the attention to the dynamics of the perturbation.

3. Dynamical equations

As mentioned in the introduction, we work in the ideal MHD approximation. Taking a time dependence of the form $\exp(\gamma t)$, for a given toroidal number n, the poloidal spectrum of the radial component of the fluid displacement is (to relevant order in a/R_0) composed of three harmonics ($m > 1$)

$$\xi^r = \sum_{l=-1}^{1} \xi^r_{m+l} {\rm e}^{{\rm i}(m+l)\vartheta - {\rm i}n\phi}.$$

We refer to $m + l$ as the poloidal mode number of the harmonic $m + l$. We further assume the harmonic with helicity m/n to resonate within the plasma, so that $q_0 < m/n < q_a$ while the lower sideband does not exhibit resonances (i.e. $(m-1)/n < q_0$). Notice that the presence of the separatrix forces the resonance of the $m + 1$ harmonic to be inside the plasma as well. The

definition of ξ^r can be extended to the vacuum region by linking the magnetic perturbation to a fictitious fluid displacement through the relation $\tilde{B}^r_\ell \propto (\ell/q-n)\xi^r_\ell$ where $\ell = m, m\pm 1$. For the sake of simplicity we write $\xi^r_\ell = \xi_\ell$.

In the region $0 < r < r_*$, the dynamics of ξ_ℓ obeys

$$\left[r^3 k_\ell^2 \xi_\ell'\right]' - r\left(\ell^2-1\right)k_\ell^2 \xi_\ell = 0, \tag{3}$$

where $k_\ell = \ell\mu - n$ with $\mu = 1/q$. Denoting with r_s the resonance of the mode m ($q(r_s) = m/n$), we impose $r_* < r_s < a$. implying $q(r_*) < q(r_s)$ and also that the single helicity m/n external kink mode is stable that is $q(r_s) < q_a$. Thus, for $r_0 < r < r_*$, the solution of (3) which is smooth at r_0 reads

$$\xi_\ell \propto \frac{1}{k_\ell}\left((r/r_0)^{\ell-1} + \frac{(r/r_0)^{-\ell-1}}{\ell-1-nq_0}\right). \tag{4}$$

The absence of currents in the vacuum region implies that $\boldsymbol{\nabla}\times\boldsymbol{B} = 0$ so that the magnetic perturbation fulfils $\tilde{\boldsymbol{B}} = \boldsymbol{\nabla}\chi$ which, expressed in terms of radial displacement, yields the Robin boundary condition [1]

$$\left.\frac{r\xi_\ell'}{\xi_\ell}\right|_{a+\epsilon} = \frac{2\ell}{\ell-nq_a} - \frac{\ell+1+(\ell-1)(a/b)^{2\ell}}{1-(a/b)^{2\ell}}, \tag{5}$$

where ϵ is an infinitesimally small positive quantity.

Focussing on the edge region where the strong gradients occur, we must account for pressure induced mode coupling. Since the plasma geometry is assumed to be circular to first approximation, we assume the poloidal spectrum to be dominated by the mth harmonic while the first neighbouring sidebands are such that $\xi^r_m \sim \varepsilon\xi^r_{m\pm1}$.

After introducing the ballooning parameter [7] $\alpha = -2R_0 p' q^2/B_0^2$, for $r_* < r < a$, the perturbation of helicity m/n conforms to the following model equations [8, 9] (although ρ' was neglected in [8])

$$\left[r^3 Q\xi_m'\right]' + r^2\frac{R_0^2\gamma^2}{B_0^2}\left(1+2q^2\right)\rho'\xi_m + n^2\frac{\alpha}{2}\sum_\pm \frac{r^{1\pm m}L_\pm}{1\pm m} = 0, \tag{6}$$

$$Q = k_m^2 + \frac{\rho R_0^2}{B_0^2}\gamma^2\left(1+2q^2\right), \tag{7}$$

where the constants $L_\pm$ account for the coupling with the neighbouring sidebands

$$\frac{L_\pm}{1\pm m} = \frac{(1\pm m)\left[2\pm m+\mathbb{C}_\pm\right]\left[2\pm m+\mathbb{B}_\pm\right]a^{-2\mp 2m}}{(\pm m-\mathbb{B}_\pm)\left[2\pm m+\mathbb{C}_\pm\right]-\left(\frac{r_*}{a}\right)^{2\pm 2m}(\pm m-\mathbb{C}_\pm)\left[2\pm m+\mathbb{B}_\pm\right]} \times \int_{r_*}^a \alpha r^{1\pm m}\xi_m \mathrm{d}r,$$

with $\mathbb{C}_\pm = r\mathrm{d}\ln\xi_{m\pm1}/\mathrm{d}r|_{r_*-\epsilon}$ and $\mathbb{B}_\pm = r\mathrm{d}\ln\xi_{m\pm1}/\mathrm{d}r|_{a+\epsilon}$. The factor $(1+2q^2)$ is the inertia enhancement arising from plasma compression in a torus which also includes the effects of sidebands [10]. For the sake of simplicity we rescale the growth rate $\gamma^2(1+2q^2)\to\gamma^2$. Equation (6) is a simplified form of the more general eigenmode equation for the mode m [8, 9] in which the perturbation has been allowed to have large radial gradients. We point out that from this general equation, neglecting pressure induced coupling terms and dropping the assumption of strong radial excursions of the fluid displacement, (3) is immediately recovered in the limit $\gamma\to 0$. It can be shown that $\xi_{m\pm1}$ and $\xi'_{m\pm1}$ are continuous at r_* so that $\mathbb{C}_\pm$ can be computed by means of (4). The computation of $\mathbb{B}_\pm$ will be discussed later. Finally, note that magnetic well effects such as those modelled in [11] have been neglected since they are of higher order compared to the coupling contributions appearing in equation (6). It is nevertheless worth mentioning that, if included, instability is expected to be slightly weakened while achieving complete suppression of Mercier modes thanks to the fact that $q > 1$.

Now, exploiting the shape of the density and pressure profiles given in (2) one can easily obtain the solution for the eigen-equation in the region of the edge gradients which reads

$$\xi_m = \begin{cases} c_0 + c_1 \arctan\left(\dfrac{k_m(r)}{\gamma/\omega_A}\right), & r_* < r < r_p, \\ d_0 + d_1 \arctan\left(\dfrac{k_m(r)\lambda^{-1}}{\gamma/\omega_A}\right), & r_p < r < a, \end{cases} \tag{8}$$

where $\omega_A = B_0/(R_0\sqrt{\rho_0})(1+2q^2)^{1/2}$ and $\lambda = \sqrt{\rho_1/\rho_0}$. The constants c_i and d_i will be determined later. Notice that if we generalise to an arbitrary q profile such that $q(r_s) = m/n$ for $r_* < r_s < a$ with $(a-r_*)/a \ll 1$, we can write the leading order solution of (6) in a form equivalent to (8) by substituting $k_m \to nsx$ where $x = (r-r_s)/r_s$ and s denotes the magnetic shear at r_s. We now have all the elements to obtain the dispersion whose derivation is discussed in the next section.

4. Dispersion relation

For the moment, we shall not specify the poloidal and toroidal mode numbers m and n. To obtain the dispersion relation, and hence the growth rate, we integrate (6) across r_p and a where

the density jumps occur yielding respectively

$$[rQ\xi_m']_{r_p} - \frac{\gamma^2}{\omega_A^2}\left(1-\lambda^2\right)\xi_m(r_p) + n^2\frac{R_0 p_0 q_p^2}{r_p B_0^2}\sum_{\pm}\frac{r_p^{\pm m}L_\pm}{1\pm m} = 0, \tag{9}$$

$$[rQ\xi_m']_a - \frac{\gamma^2}{\omega_A^2}\lambda^2\xi_m(a) = 0, \tag{10}$$

where $[A]_r = A(r+\epsilon) - A(r-\epsilon)$ with $\epsilon \to 0$. Notice that in the neighbourhood of the separatrix where $q=\infty$ the quantity k_ℓ is well defined at the boundary for any harmonic since $\mu(a)\to 0$.

Firstly, one easily sees that $[r^3 Q\xi_m']_{r_*} = 0$, thus implying that ξ_m' and ξ_m are continuous at r_*, so that

$$\mathbb{C}_m \equiv \left.\frac{r\xi_m'}{\xi_m}\right|_{r_*-\epsilon} = \left.\frac{r\xi_m'}{\xi_m}\right|_{r_*+\epsilon} = \left.\frac{\gamma}{\omega_A}\times\frac{(rk_m')/Q}{c_0/c_1+\arctan\left[k_m/(\gamma/\omega_A)\right]}\right|_{r_*},$$

where the value of $\mathbb{C}_m$ is obtained from (4) in analogy to $\mathbb{C}_\pm$. The relation above is inverted to get the ratio c_0/c_1.

Equations (8) and (10) yield

$$\frac{d_0}{d_1} = \left[\frac{\lambda r k_m'\gamma/\omega_A}{k_m^2\mathbb{B}_m - \lambda^2\gamma^2/\omega_A^2} - \arctan\left(\frac{k_m\lambda^{-1}}{\gamma/\omega_A}\right)\right]_{a-\epsilon},$$

where $\mathbb{B}_m = r\xi_m'/\xi_m|_{a+\epsilon}$ and is obtained from (5) by setting $\ell = m$. Notice that because of the density step at $r=a$ in general $r\xi_m'/\xi_m|_{a-\epsilon} \neq r\xi_m'/\xi_m|_{a+\epsilon}$ with the difference expressed by (10). Hence, the eigensolution of the mode m in the region of strong gradients is completely determined, and we can now proceed to derive the dispersion relation.

Under the condition that ξ_m is continuous at r_p [9], the following dispersion relation is produced from (9):

$$\frac{\gamma}{\omega_A}(rk_m')_{r_p}\left(\frac{\lambda}{\frac{d_0}{d_1}+\arctan\left[k_m(r_p)\lambda^{-1}/(\gamma/\omega_A)\right]} - \frac{1}{\frac{c_0}{c_1}+\arctan\left[k_m(r_p)/(\gamma/\omega_A)\right]}\right) - \frac{\gamma^2}{\omega_A^2}\left(1-\lambda^2\right) + \left(n\frac{R_0}{r_p}q_p^2\beta\right)^2 U = 0, \tag{11}$$

where we defined $\beta = p_0/B_0^2$ with $q_p = q(r_p)$ and

$$U = \sum_{\pm}\frac{2(1\pm m)\left[2\pm m+\mathbb{C}_\pm\right]\left[2\pm m+\mathbb{B}_\pm\right](r_p/a)^{2\pm 2m}}{(\pm m-\mathbb{B}_\pm)\left[2\pm m+\mathbb{C}_\pm\right] - (r_*/a)^{2\pm 2m}(\pm m-\mathbb{C}_\pm)\left[2\pm m+\mathbb{B}_\pm\right]}.$$

We first note that ignoring the presence of a separatrix, the dispersion relation for external kink modes is immediately retrieved by letting $\lambda = 1$, $\beta = 0$ and $r_* \to r_p \to a$ in (11), which eventually gives $c_0/c_1 = d_0/d_1$.

In the neighbourhood of the marginal boundaries, the growth rate is small enough so that contributions of order γ^2 are negligible. If the resonance m/n occurs at $r_s < r_p$ we obtain

$$\frac{\gamma}{\omega_A} \approx -\pi\left[\left(n\frac{R_0}{r_p}q_p^2\beta\right)^2\frac{U}{(rk_m')_{r_p}} + \frac{k_m(a)}{1+\left.\frac{rk_m'}{k_m}\right|_a\mathbb{B}_m^{-1} - \frac{k_m(a)}{k_m(r_p)}}\right], \tag{12}$$

whereas for the case $r_p < r_s < a$ one has

$$\frac{\gamma}{\omega_A} \approx -\frac{\pi}{\lambda}\left[\left(n\frac{R_0}{r_p}q_p^2\beta\right)^2\frac{U}{(rk_m')_{r_p}} - \frac{k_m(r_*)}{1+\left.\frac{rk_m'}{k_m}\right|_{r_*}\mathbb{C}_m^{-1} - \frac{k_m(r_*)}{k_m(r_p)}}\right]. \tag{13}$$

It will be shown later that a window in q_a can be found within which the mode becomes unstable. The largest value of the growth rate is typically attained when the resonance coincides with the location of the step in pressure. Hence, at this location and assuming that γ/ω_A is sufficiently small, we may write

$$\frac{\gamma}{\omega_A}(1+\lambda) \approx -\frac{\pi}{2}\left(n\frac{R_0}{r_p}q_p^2\beta\right)^2\frac{U}{(rk_m')_{r_p}}. \tag{14}$$

Up to this point the discussion has been left sufficiently generic such that no specific helicities have been taken into account. Now, we study in detail the behaviour of the $m=2$, $n=1$ mode. This is detailed in the next section.

5. The $m=2$, $n=1$ mode

Let us first note that in proximity of a the radial fluid displacement obeys equation (3). Because of the logarithmic divergence of the safety factor at the edge, we may assume that the resonance of the the $m+1$ harmonic occurs at $r=a$, that is $k_{m+1}(a)=0$. Upon introducing the variable $y=(r-a)/a$, near this point we write

$$\xi_{m+1} \propto 1 + Ay^\nu,$$

where A is a constant to be determined later and $\nu > 0$. Close to the resonance, we are allowed to approximate $k_{m+1} \propto y$. When this form of ξ_{m+1} is plugged into (3) we obtain

$$A\nu\left(\nu+1\right)y^{\nu-2} - \left[\left(m+1\right)^2 - 1\right] = 0,$$

which is solved by setting $\nu = 2$, meaning that the eigenfunction approaches the resonance with vanishing radial derivative (the expression of A follows accordingly). Hence, the presence of a separatrix dictates that $\mathbb{B}_+ = 0$.

Now, for the specific case of $m = 2$ and $n = 1$, it is straightforward to see from (4) that $\mathbb{C}_- = 0$, so that one has $L_- = 0$. This, therefore, implies that

$$U = \frac{12\left(4+\mathbb{C}_+\right)\left(r_p/a\right)^6}{4+\mathbb{C}_+ - 2\left(2-\mathbb{C}_+\right)\left(r_*/a\right)^6},$$

where, exploiting the fact that $q(r_*) = q_0(r_*/r_0)^2$, the quantity $\mathbb{C}_+$ can be expressed as

$$\mathbb{C}_+ = 2 + 12\left(\frac{1-\left(r_0/r_*\right)^6 - \frac{q_0}{2}\left(1-\left(r_0/r_*\right)^4\right)}{\left[3-q\left(r_*\right)\right]\left[2-q_0+\left(r_0/r_*\right)^6\right]}\right).$$

Since we take $1 < q_0 < 2$ and $q(r_*) < 2$ by hypothesis, it is easily seen that the term in brackets on the right-hand-side of the expression above is positive so that $\mathbb{C}_+ > 2$. It thus follows that $U > 0$. Hence, by comparing with (14) we see that if the $2/1$ resonance occurs at the location of the step of the pressure profile the mode is always unstable. We are thus led to infer that there might be situations in which even an infinitesimally small gradient in pressure is sufficient to trigger the instability. If $r_*/a = 1-h$ and $r_p/a = 1-h/2$ with $h \ll 1$ the expression for the growth rate can be further simplified leading to

$$\frac{\gamma}{\omega_A} \approx \frac{16\pi}{1+\lambda}\left(\frac{R_0}{r_p}\beta\right)^2\left(1+\frac{4}{\mathbb{C}_+}\right). \tag{15}$$

An example of the magnitude of the growth rate computed with experimentally relevant parameters is given in figure 2. A window of instability opens exactly when the resonance of the $2/1$ mode occurs in proximity of r_p, namely the position of the step of the pressure profile. In an experimental situation when the plasma current is ramped up, the location of r_s moves from the core region towards the edge (i.e. left to right in figure 2) so that, following the discussion below (15), we can expect that an instability always occurs if the location of the resonance aligns with that of the edge pressure gradients. Furthermore, one sees that even with modest edge gradients the perturbation can grow on quite fast time-scales of the order of few milliseconds or less. We shall point out, nonetheless, that these are much slower than those associated with purely current driven external kink modes in limited geometries [1].

The eigenfunction of the dominant $m = 2$ harmonic corresponding to the case marked by the star of figure 2 is shown in figure 3. The perturbed displacement is larger in the region of the edge gradients, although it remains appreciably different from zero in the core. In particular, we see that $\xi_2(a) \neq 0$.

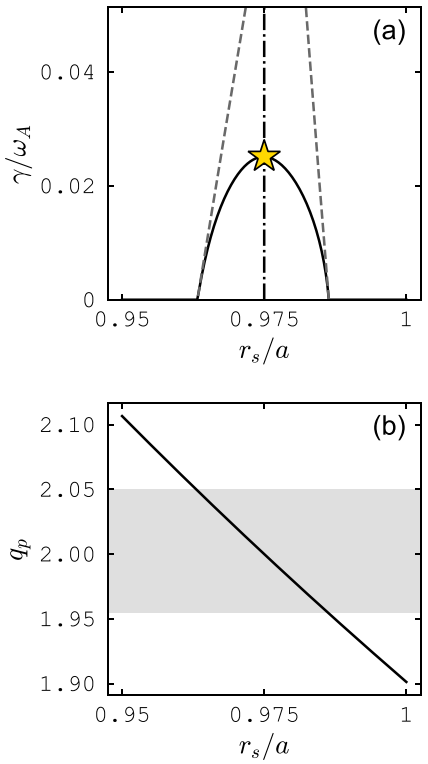

Figure 2. (a) Growth rate for the $2/1$ mode as a function of its resonant position computed with parameters $q_0 = 1.3$, $r_*/a = 0.95$, $r_p/a = 0.975$, $a/R_0 = 1/4$, $\beta = 0.005$, $\rho_1/\rho_0 = 0.2$ and $a/b \to 0$. In (a) the position of the step of the pressure profile is marked by the vertical dot-dashed line whereas the two dashed Grey lines are obtained from (12) and (13); the star denotes the approximated growth rate computed from (15). The shaded area in (b) highlights the corresponding instability window in q_p.

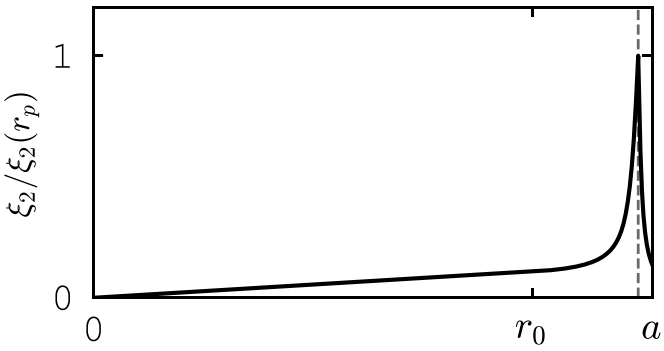

Figure 3. Shape of the eigenfunction of the $m = 2$ harmonics computed with the same parameters of figure 2 with the mode resonance coinciding with the position of the step in the pressure profile (i.e. $r_s = r_p$, star in figure 2). The dashed vertical line marks the radius r_p.

Larger growth rates are expected to yield bigger values of the fluid displacement at the boundary.

Although our analysis has been carried out with a rather *'rigid'* safety factor, we point out that the width of the instability window, either in r_s or q_a, can be widened both by enhancing the edge pressure gradient or by reducing the local magnetic shear in the region $r_* < r < a$. This can be indeed

inferred from (12) and (14) by noting that $k'_m \sim s$ with s the local shear in the gradient region, i.e. the lower the shear the higher the instability drive.

6. Conclusions

To summarise, in this work we addressed the problem of the excitation of global instabilities in a diverted configuration, when single helicity current driven external kink modes are intrinsically stable. The analysis has been carried out by exploiting the presence of strong density and pressure gradients near the plasma edge. This induces an *infernal-type* mode coupling [8], thus allowing for the onset of otherwise stable global perturbations.

We found that the onset of the instability occurs when the resonance of the dominant harmonic gets closer to the region of strong gradients, that is when the field line bending stabilisation associated with the magnetic shear is weakened. The structure of the eigenfunction, although exhibiting a sharp rise close to the edge, maintains a rather global character being different from zero all the way across the plasma column.

Growth rates computed by using physical parameters, which are not too far from those characterising typical tokamak experiments, fall within the range of few milliseconds even with modest edge radial gradients, thus indicating a fairly fast growth. The onset of the instability appears sharply when the parameter q_p, namely the value of the safety factor at the location of the pressure step, approaches the value 2 in line with the experimental evidence. In our model, the narrowness of the region of instability is because of the choice of the (simplified) equilibrium profiles. Nonetheless, it may be widened by reducing the local magnetic shear, this being possible through bootstrap contributions.

Although our model has been developed within the ideal MHD framework, we point out that a further worsening of stability can be produced by including resistive effects, which are expected to become important close to the ideal marginal points and in regions where the plasma temperature is small. The inclusion of these correction to the dynamics of the $q_{95} = 2$ limit is more likely addressed via numerical approaches [12]. Since this work has been focussing on global (i.e. $n \sim 1$) disturbances only, the stability of large-n perturbations such as ballooning modes has not been analysed. We nevertheless point out that β and r_* may be tuned to stabilise localised perturbations [13] while the global $2/1$ mode may still be present (see equation (15)). We finally envisage that this framework may also be extended to model pressure driven core MHD instabilities to give, at least, a qualitative description of their behaviour.

Data availability statement

No new data were created or analysed in this study.

Acknowledgments

This work has received funding from Enabling Research grant on Operational Limiting Plasma Instabilities (CdP-FSD-AWP21-ENR-03) and from EPSRC Energy Programme (Grant EP/W006839/1). This work has been carried out within the framework of the EUROfusion Consortium, funded by the European Union via the Euratom Research and Training Programme (Grant Agreement No. 101052200—EUROfusion). Views and opinions expressed are however those of the author(s) only and do not necessarily reflect those of the European Union or the European Commission. Neither the European Union nor the European Commission can be held responsible for them. This work was supported in part by the Swiss National Science Foundation.

ORCID iDs

D Brunetti 0000-0001-8650-3271
J P Graves 0000-0002-7959-7959
C J Ham 0000-0001-9190-8310
S Saarelma 0000-0002-6838-2194

References

[1] Shafranov V D 1970 *Sov. Phys.-Tech. Phys.* **15** 175
[2] Turnbull D *et al* 2016 *J. Plasma Phys.* **82** 515820301
[3] Zakharov L E 2008 *Phys. Plasmas* **15** 062507
[4] Zakharov L E, Galkin S A and Gerasimov S N (JET-EFDA Contributors) 2012 *Phys. Plasmas* **19** 055703
[5] Piovesan P *et al* 2014 *Phys. Rev. Lett.* **113** 045003
[6] Huysmans G T A 2005 *Plasma Phys. Control. Fusion* **47** 2107
[7] Connor J W, Hastie R J and Taylor J B 1978 *Phys. Rev. Lett.* **40** 396
[8] Hastie R J and Hender T C 1988 *Nucl. Fusion* **28** 585
[9] Brunetti D, Graves J P, Lazzaro E, Mariani A, Nowak S, Cooper W A and Wahlberg C 2018 *Nucl. Fusion* **58** 014002
[10] Glasser A H, Greene J M and Johnson J L 1976 *Phys. Plasmas* **19** 567
[11] Wilson H R and Miller R L 1999 *Phys. Plasmas* **6** 873
[12] Sabbagh S A, Hughes M H, Phillips M W, Todd A M M and Navratil G A 1989 *Nucl. Fusion* **29** 423
[13] Wesson J A and Sykes A 1985 *Nucl. Fusion* **25** 85